

ANGLE-DEPENDENT REFLECTANCE OF ISOTEXTURED SILICON

Aina Alapont Sabater¹, Johannes M. Greulich¹, Nico Tucher¹, Benedikt Bläsi¹, Stefan W. Glunz^{1,2}

¹Fraunhofer Institute for Solar Energy Systems ISE, Heidenhofstraße 2, 79110 Freiburg, Germany

²Albert-Ludwigs-University Freiburg, Laboratory for Photovoltaic Energy Conversion, Georges-Köhler-Allee 105, 79110 Freiburg, Germany

Telephone: +49 761 4588 5075, e-mail: aina.alapont.sabater@ise.fraunhofer.de

ABSTRACT: Multicrystalline silicon (mc-Si) is the workhorse of photovoltaics with a market share above 60%, being acidic textured (isotextured) silicon the standard. For optical simulations, the spherical caps model is widely applied, but it was reported that it does not correctly describe the angular dependence of reflection. In this work, our first objective is to verify this. Secondly, we want to obtain an improved model for optics of isotextured mc-Si wafers and solar cells able to describe the light trapping properties of cells and modules correctly. We investigate the reflectance of isotextured silicon by varying the angle of incidence of the light between 8° and 80°. We perform measurements of nine isotextured samples, obtaining reflectance curves with a similar shape, but they differ by up to 60%_{abs} from previously published data. The first simulations are performed using the spherical caps model, which is shown to be inaccurate to describe the angle-dependent reflectance of isotextured silicon. In the second set of simulations we vary the texture morphology, reducing the deviations of the simulation from the measurement from 8% to 1.2% for incident angles smaller than 60°. We conclude that alternative morphologies are worth doing further research.

Keywords: Silicon Solar Cell, Multicrystalline Silicon, Optical Properties, Simulation, Light trapping

1 INTRODUCTION

Multicrystalline silicon (mc-Si) with an isotextured front surface, i.e. isotropically etched silicon by hydrofluoric acid (HF) and nitric acid (HNO₃) [1], has a market share in the photovoltaic industry of more than 60% and is expected to keep a share well above 40% for the next ten years [2]. Simulation is the basis for a thorough analysis of the performance of the isotexture including light trapping in the cell and especially in the module. For optical simulations of isotextured silicon solar cells, the spherical caps model was proposed [3] and is widely used. By adjusting the opening angle as characteristic parameter this model is capable of describing the hemispherical reflectance [4] and hemispherical transmittance [5] for normally incident light. However, it lacks a simple and accurate description of its angular dependence [3, 6], which is of utmost importance for the light trapping within the solar cell and within the module.

In this paper we present angle-dependent reflectance measurement results of isotextured silicon which show a different behaviour than previously published data [3, 5, 6]. We also evaluate different isotexture morphologies to look in further detail at the reflectance for different angles of incidence of the light. We present the corresponding simulations applying alternative morphologies and compare our results with the simulations using the spherical caps approach.

This work presents a new model for the optical simulation of isotextured silicon, worthy of further investigation, since the accurate description of angle-dependence would be a step forward in the solar cell simulation.

2 EXPERIMENTAL

We work with nine different mc-Si wafers, which are wet-chemically textured. Four of them were processed at Fraunhofer ISE at two different process speeds and two different acid concentrations, resulting in the formation

of four different textures: “strong” (see Figure 1a), “medium” (see Figure 1b) and two “weak”. Additionally, four wafers were kindly provided by the Australian National University (ANU), also with different textures, and the SCHMID Group sent us a textured wafer with “DW PreTex” treatment [7].

As representative group, we present in this paper the results of three samples with different textures: “strong” from ISE (see Figure 1a), “medium” from ISE (see Figure 1b) and “weak” from the ANU (see Figure 1c). The planar wafer, used as reference, is a polished float zone (FZ). From each wafer we cut two samples in the dimensions of 2x3.3 cm² and 3.3x4.5 cm².

A spectrophotometer with an Ulbricht sphere

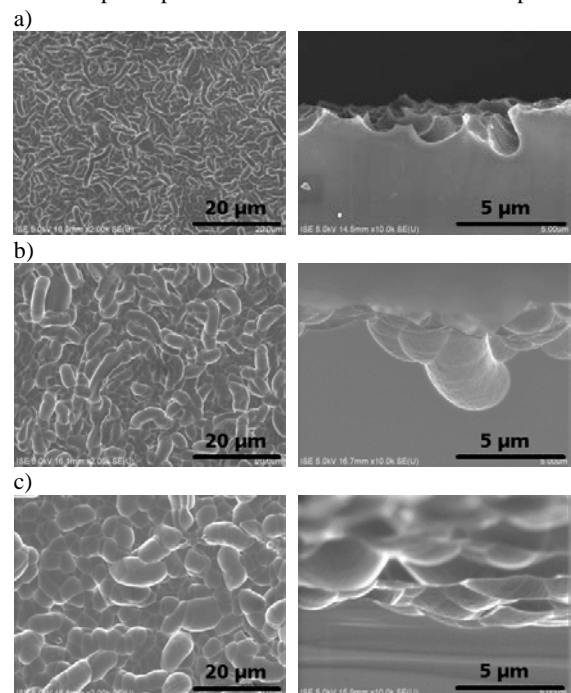


Figure 1: Scanning electron micrograph of the (a) strong, (b) medium and (c) weak isotextured samples. Left: top view; Right: cross section.

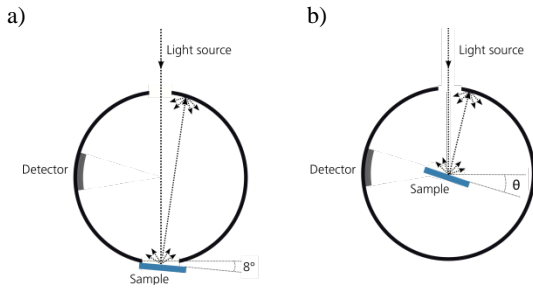


Figure 2: Sketch of the two measurement setups.

(Fourier-Spectrometer), with diameter of 20 cm is used for the measurements. The reference measurement is performed as shown in Figure 2a: sample mounted externally at the sphere at an angle of the incident light of 8°. The other measurements are performed with the sample center mounted within the Ulbricht sphere (see Figure 2b), which is rotated, thereby increasing the angle of incidence of the light θ .

In order to get the most accurate measurements, i.e. to avoid that the reflected light on the sphere strikes again the sample, the sample should be as small as possible. Meanwhile, the sample has to be large enough so that the whole light beam strikes it. Considering these two requirements, we use the small samples for incident angles $\theta \leq 60^\circ$ and the large samples for $\theta \geq 60^\circ$.

3 SIMULATION

We perform three different sets of optical simulations, which are described below. All of them apply 3D geometric optics (ray tracing) and the transfer matrix method. The incident angle θ is varied between 0 and 88°.

3.1 Spherical caps

The first set of simulations are performed using the Module Ray Tracer (MRT) by PV Lighthouse [8], using refractive index data for silicon from Ref. [9]. The simulations of the hemispherical reflectance are performed with 10^6 rays and wavelengths between 300 and 1000 nm in steps of 10 nm. The MRT uses the spherical caps approach. As shown in Figure 3, the morphology is described as an inverted spherical cap by the characteristic angle ω_c .

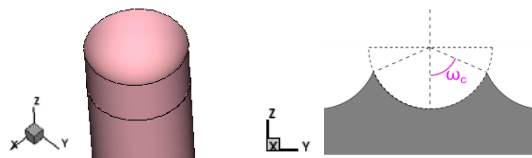


Figure 3: Symmetry element and characteristic angle ω_c of the isotexture in the spherical cap approach.

3.2 Quadratic grid

The second and third sets of numerical simulations are performed using Sentaurus Device [10], since this software allows us more flexibility, e.g. by varying the texture morphology and the ray randomization algorithms. We use in this case a spherical caps morphology, out of which a pillar with quadratic cross section is cut, resulting in the symmetry element shown in Figure 4, also described by the characteristic angle ω_c .

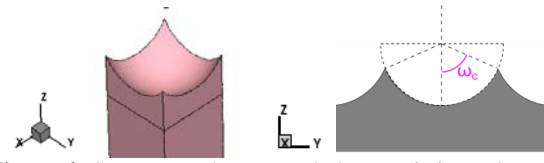


Figure 4: Symmetry element and characteristic angle ω_c of the isotexture in the quadratic grid approach. The cross section corresponds to a cut through the centre of the symmetry element.

3.3 Tub form

As depicted in scanning electron microscopy (SEM) images in Figure 1, the morphology of isotextured silicon appears to resemble a tub form. We implemented this as optical model by defining two characteristic parameters: the characteristic angle ω_c and the characteristic length L_c (see Figure 5). Furthermore, the weaker the texture is, the shorter is L_c , the shape being more rounded and the geometry more similar to a spherical cap.

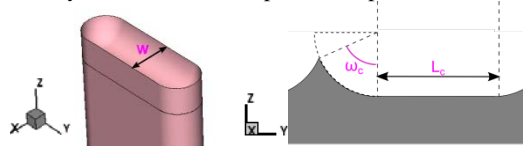


Figure 5: Symmetry element, width w , characteristic angle ω_c and characteristic length L_c of the isotexture in the tub form approach.

4 RESULTS

First, we compare our measurement results of the three samples with data from Ref. [3]. As shown in Figure 6, our measurements show a much less pronounced dependence on θ than the measurements from Ref. [3]. The same holds not only for the samples fabricated at Fraunhofer ISE, but also for our measurements at samples from the original batch of Ref. [3] that were kindly provided by the ANU. The differences in R are above 27%_{abs} for angles greater than 75°. After discussing this discrepancy with the authors of that study, we conclude that an error occurred in part of the data from Ref. [3], besides the error when determining the characteristic angle ω_c of the texture that

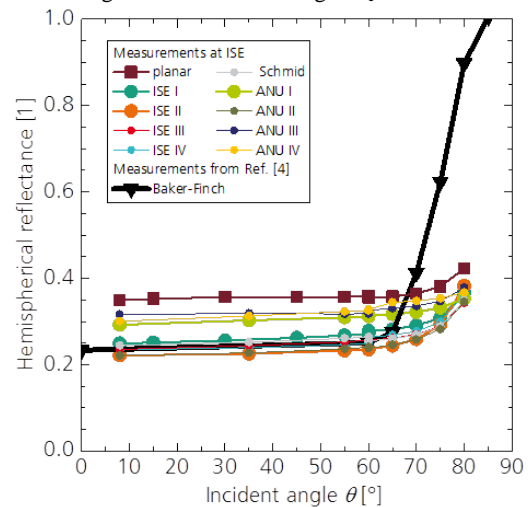


Figure 6: Reflectance R of isotextured silicon for $\lambda = 600$ nm for two cases: 1) Measurements of this work performed at ISE; 2) Measurements from Baker-Finch et al. [3].

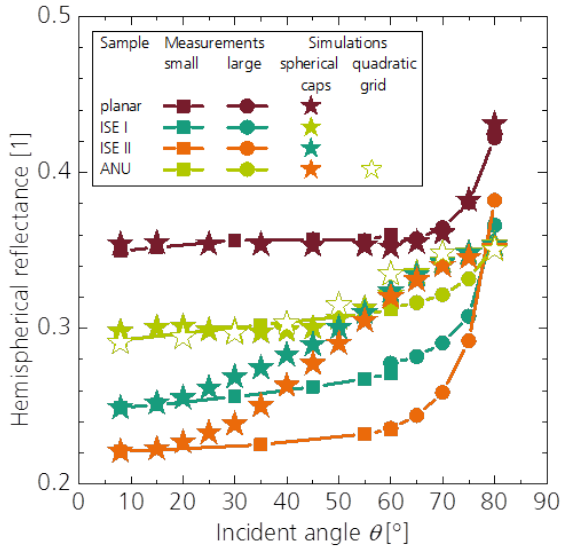


Figure 7: Simulated (stars) and measured (lines) reflectance R for $\lambda = 600$ nm for one planar and three isotextured silicon samples.

the authors recently reported [5].

Second, we focus on the spherical caps model, using the MRT by PV Lighthouse, and compare it to our measurements. The simulated and measured reflectance of the planar sample, used as reference, are in close agreement with deviations smaller than $0.9\%_{\text{abs}}$ (see Figure 7), which indicates that both the experimental setup as well as the simulation scheme work properly. We adjust ω_c in the MRT, so that the simulated hemispherical reflectance R_{sim} matches the measured reflectance R_m at $\theta = 8^\circ$, obtaining $\omega_c^{\text{ISE I}} = 60^\circ$, $\omega_c^{\text{ISE II}} = 66^\circ$, $\omega_c^{\text{ANU}} = 52^\circ$. The next simulations are carried out using this characteristic value, and varying the angle of incidence θ between 8 and 80° . The results shown in Figure 7 reveal a high discrepancy; differences in R are above $5\%_{\text{abs}}$ for $\theta = 60^\circ$ for the sample ISE I and above $8\%_{\text{abs}}$ for $\theta = 60^\circ$ for the sample ISE II. We also simulate the sample from the ANU with the quadratic grid approach (see Figure 7), obtaining very similar

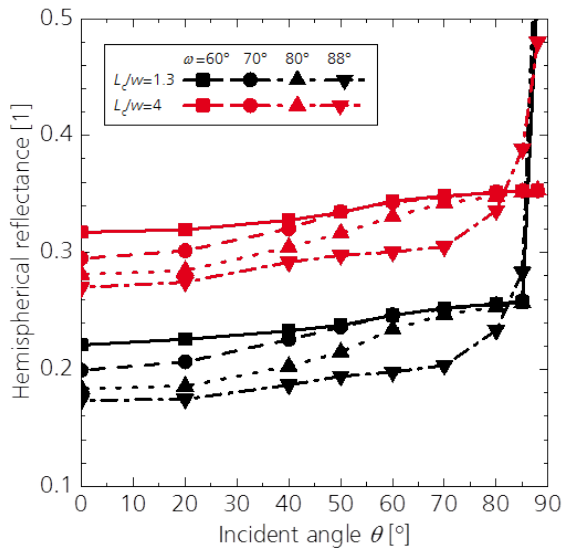


Figure 8: Simulated reflectance R for $\lambda = 600$ nm of the tub geometry including a variation of the characteristic parameters ω_c and L_c/w for fixed $\varphi = 0^\circ$.

results to those using the spherical caps approach.

Third, we test the tub form model in order to analyse and understand better this new approach. To that end, we analyse the influence of the characteristic parameters on the reflectance. As shown in Figure 8, the greater the ratio L_c/w and the smaller the ω_c , the higher the reflectance R . For small ω_c ($60^\circ < \omega_c < 70^\circ$) the reflectance consists of two straight lines with a sharp change in the slope at $\theta = 85^\circ$. When ω_c increases up to 88° , R is a curved line.

Furthermore, we perform another variation, this time of the azimuth φ (described in Figure 9) and the characteristic length L_c , for a fixed $\omega_c = 88^\circ$.

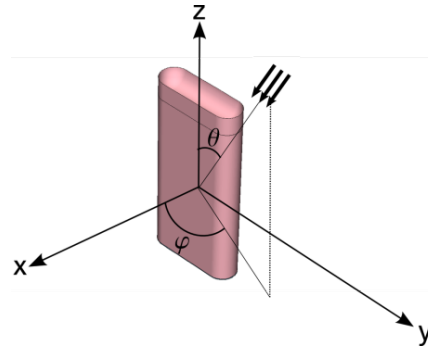


Figure 9: Definition of the incident angle or zenith θ and azimuth φ .

Like in the previous case, the reflectance is higher when the value of L_c/w increases (see Figure 10). For small φ , the reflectance only rises with the incident angle θ . However, for larger φ the reflectance rises and falls with the variation of θ .

At this point, we perform the simulations using the tub form approach and compare them to the measurements. As for the previous simulations, we adjust the characteristic parameters, obtaining the values shown in Table 1. Other combinations of L_c/w and ω_c might be possible to reach the same reflectance at 600nm for $\theta = 8$. Because isotextured silicon is irregular (see Figure 1) and every tub has a different orientation, we simulate the

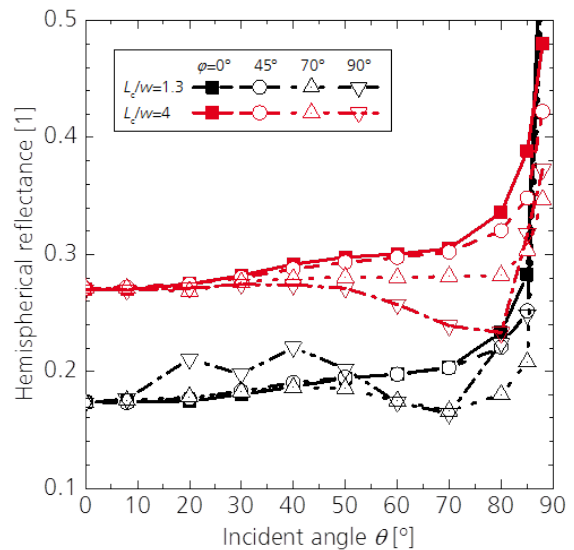


Figure 10: Simulated reflectance R for $\lambda = 600$ nm of the tub geometry including a variation of azimuth φ and characteristic length L_c for fixed characteristic angle $\omega_c = 88^\circ$.

whole range of φ (from 0 to 90°) and calculate an averaged reflectance.

Table 1: Hemispherical reflectance and fitting ratio L_c/w and characteristic angle ω_c for the three isotextured samples for the tub geometry.

Sample	$R(600\text{nm}, \theta = 8^\circ)$ [%]	L_c/w [-]	ω_c [°]
ISE I	24.9	3.2	88
ISE II	22.1	2.2	88
ANU	29.2	4.7	88

The results depicted in Figure 11 show a good agreement for the planar sample for all angles, as well as for the isotextured samples for incident angles of up to 60°: in this region the difference between simulated and measured results is always below 1.2%_{abs}. From this point the behavior of the simulated reflectance R_{sim} differs gradually from the measured reflectance R_{m} . To see more clearly the difference between the two approaches (spherical caps and tub form) we plot in Figure 11 again the reflectance obtained with the spherical caps model for the sample ISE II.

5 DISCUSSION

The angle-dependence is not well described by the spherical caps model, resulting in an overestimation of the reflectance (see Figure 7) of up to 8%_{abs} for incident angles around 60°. For isotextured samples with poor optical properties, which exhibit a reflectance of almost 30% for an incident angle of 8°, the discrepancies between measurements and simulations with the spherical caps model are smaller (below 2%_{abs}). Nevertheless, it is in industry's interest to produce solar cells with good optical properties, as the samples ISE I and ISE II with only 25% and 22% reflectance for $\theta = 8^\circ$ respectively. The same argument applies to the quadratic grid approach. This presents similar results as the spherical caps approach and consequently is also inaccurate.

In the range $0 < \theta < 60^\circ$, the tub form approach describes quite accurately the angle-dependent

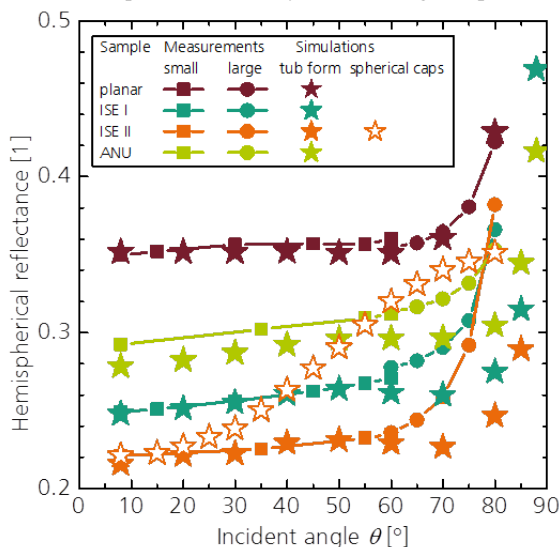


Figure 11: Simulated (stars) and measured (lines) reflectance R for $\lambda = 600$ nm for one planar and three isotextured silicon samples.

reflectance of isotextured silicon (see Figure 11). The results show discrepancies much smaller than by using the spherical caps approach. Furthermore, solar cells are not installed alone, but they are encapsulated with ethylene vinyl acetate (EVA) and glass. Due to the refractive index of these two layers, the incident angle is reduced; reaching rarely values over 50° on the solar cell. For this important range, the tub approach represents an improvement compared to the spherical caps approach. Nevertheless, the complete range of incident angles up to 90° is important for light trapping within the module. Further research is required to improve the optical models in the range of incident angles between 60° and 90°.

6 SUMMARY AND CONCLUSION

We have presented an optical analysis of isotextured silicon, studying the angle-dependent reflectance. Our work has been developed in three parts. First, we have compared our measurements of nine different isotextured samples with published data [3]. We revealed that the published data are partly inaccurate and we laid the foundations for a thorough analysis of isotextured silicon by generating reliable reflectance data.

Second, we have performed simulations by using the Module Ray Tracer by PV Lighthouse, where the spherical caps model was implemented. Comparing the simulated results with the measurements, we have demonstrated that this model is not able to describe the measured reflectance when the incident light is not perpendicular to the cell, reaching differences between simulated reflectance R_{sim} and measured reflectance R_{meas} above 8%_{abs} for well-textured samples.

Third, we have analysed two more morphologies of the simulation model. We have shown a superior match between measurements and simulations using the tub morphology for incident angles from 0 to 60°. The difference $R_{\text{sim}} - R_{\text{meas}}$ is reduced to 1.2%_{abs} for incident angles θ from 0 to 60°. We conclude that the new tub form approach is promising and that further research is required for further improvements.

ACKNOWLEDGEMENTS

This work was partly funded by the German Federal Ministry for Economic Affairs and Energy within the research project "BiZePS" (contract number 0325909).

The authors would like to thank their colleagues at ISE for their work, Simeon C. Baker-Finch and Keith R. McIntosh for the discussion and the SCHMID group for providing a textured sample with DW PreTex treatment.

Aina Alapont Sabater gratefully acknowledges the support by scholarship funds from the Deutsche Bundesstiftung Umwelt.

REFERENCES

- [1] Sarti, D., Le, Q. N., Bastide, S., Goer, G., & Ferry, D., "Thin industrial multicrystalline solar cells and improved optical absorption," *Proceedings of the 13th European PV Solar Energy Conference*, pp. 25–28, 1995.

- [2] “International Technology Roadmap for Photovoltaic (ITRPV): 2015 Results including maturity reports,” Seventh Edition, Oct. 2016.
- [3] S. C. Baker-Finch, K. R. McIntosh, and M. L. Terry, “Isotextured Silicon Solar Cell Analysis and Modeling 1: Optics,” *IEEE J. Photovoltaics*, vol. 2, no. 4, pp. 457–464, 2012.
- [4] J. Greulich *et al.*, “Optical Simulation and Analysis of Iso-textured Silicon Solar Cells and Modules Including Light Trapping,” *Energy Procedia*, vol. 77, pp. 69–74, 2015.
- [5] K. R. McIntosh, T. G. Allen, S. C. Baker-Finch, and M. D. Abbott, “Light Trapping in Isotextured Silicon Wafers,” *IEEE J. Photovoltaics*, vol. 7, no. 1, pp. 110–117, 2017.
- [6] K. R. McIntosh, M. D. Abbott, and B. A. Sudbury, “Ray Tracing Isotextured Solar Cells,” *Energy Procedia*, vol. 92, pp. 122–129, 2016.
- [7] SCHMID Group | Gebr. SCHMID GmbH, *SCHMID develops new process for the texturing of diamond-wire-cut multi-wafers: Press release, Feb 2, 2017.*
- [8] *PV Lighthouse: Module Ray Tracer*. [Online] Available: <https://www.pvlighthouse.com.au>. Accessed on: Jun. 07 2017.
- [9] M. A. Green, “Self-consistent optical parameters of intrinsic silicon at 300K including temperature coefficients,” *Solar Energy Materials and Solar Cells*, vol. 92, no. 11, pp. 1305–1310, 2008.
- [10] Synopsys, “Sentaurus™ Device User Guide: vI-2013.12,”